

# Determination of radioactivity levels and associated hazards of coastal sediment from south east coast of Tamil Nadu with statistical approach

S. Sivakumar<sup>1</sup> · A. Chandrasekaran<sup>2</sup> · G. Senthilkumar<sup>3</sup> · M. Suresh Gandhi<sup>4</sup> · R. Ravisankar<sup>5</sup>

Received: 27 April 2016 / Accepted: 23 February 2017 / Published online: 24 April 2017  
© Shiraz University 2017

**Abstract** The concentration of  $^{238}\text{U}$ ,  $^{232}\text{Th}$  and  $^{40}\text{K}$  in sediment samples collected from Thazhankudato Kodyakkarai along the east coast of Tamil Nadu, India was measured using  $\gamma$ -spectrometry. Measured mean activity concentrations are 3.3, 40.45 and 389.28 Bq kg<sup>-1</sup> for  $^{238}\text{U}$ ,  $^{232}\text{Th}$  and  $^{40}\text{K}$ , respectively. The average activity concentration of  $^{232}\text{Th}$  is slightly higher than the world average value. The radiation hazards such as radium equivalent activity, absorbed gamma dose rates in air, the annual gonadal dose equivalent, annual effective dose equivalent, external hazard index, internal hazard index, representative level index and excess lifetime cancer risk associated with the radionuclides were calculated. Heat production rate of sediments and spatial distribution of radionuclides is studied. The multivariate statistical analysis, such as Pearson correlation, principal component and cluster analysis were applied to know the existing relation between radiological variables. From the analysis, the radioactivity levels in sediment samples do not pose any

environmental health problem. Thus, the presented data provide a general background of the detectable radionuclides for the study area and can be helpful in future epidemiological studies.

**Keywords** Sediments · Gamma ray spectrometry · Radiation hazards · Multivariate statistical analysis

## 1 Introduction

Man is continuously exposed to ionizing radiation from naturally occurring radioactive materials (NORM). The origin of these materials is the Earth's crust. The exposure of ionizing radiations from natural sources such as soil, sediments and rocks, cosmic rays entering the earth's atmosphere. The radiological implication of these radionuclides is due to the gamma ray exposure of the body and irradiation of lung tissue from inhalation of radon and its daughters. The assessment of gamma radiation dose from natural sources is of particular importance as natural radiation is the largest contributor to the external dose of the world population (UNSCEAR 1988).

Many areas in the world such as Australia, Brazil, China, India, Iran, and Japan possess high levels of natural radiation. In the recent years, studies on the high background radiation areas in the world have been of prime importance for risk estimation due to long term low-level whole body exposures to the public. The high radiation levels are due to the presence of large quantities of naturally occurring radioactive minerals in the rocks, soils, sediments, etc. Among the various geological formations, sediment plays a predominant role in aquatic radioecology and plays a role in accumulating and transporting contaminants within the geographic area (Suresh Gandhi et al.

✉ R. Ravisankar  
ravisankarphysics@gmail.com;  
chandrasekarana@ssn.edu.in

<sup>1</sup> Department of Physics, KL University, Green Fields, Vaddeswaram, Guntur Dist. 522 502, Andhra Pradesh, India

<sup>2</sup> Department of Physics, SSN College of Engineering, Kalavakkam, Chennai 603110, Tamilnadu, India

<sup>3</sup> Department of Physics, University College of Engineering (A Constituent College of Anna University, Chennai), Arni, Thiruvannamalai Dist. 632326, Tamilnadu, India

<sup>4</sup> Department of Geology, University of Madras, Guindy Campus, Chennai 600 025, Tamilnadu, India

<sup>5</sup> Post Graduate and Research Department of Physics, Government Arts College, Thiruvannamalai 606603, Tamilnadu, India

2014). Therefore, measurements of natural radioactivity in sediments are of a great interest for many researchers throughout the world, which led to worldwide national surveys in the last two decades. Natural radioactivity measurements in coastal sediments in different parts of the world were reported by many authors (Saad and Al-Azmi 2002; Arogunjo et al. 2004; Mohanty et al. 2004; Akram et al. 2006; Orgun et al. 2007; Uosif et al. 2008; Alatise et al. 2008; Zare et al. 2012; Tari et al. 2013).

The study area chosen for the present work is due to recent industry developments during the last two decades in Cuddalore, Karaikal, Nagapattinam and Velankanni coastal towns include offshore oil production, chemical, fertilizer processing plants and more than 300 small scale industries, all located in this region. The study area is also drained by the tributaries of river Cauvery, which runs through many industrial towns and its tributaries (Stephen-Pichaimani et al. 2008).

The main objective of the work is to (1) determine the concentration of radionuclides in sediment samples, (2) calculate the radiation hazard associated with radionuclides, (3) determine the relationship between the radioactive variables using multivariate statistical analysis.

## 2 Materials and Methods

### 2.1 Geological Formation of Study Area

The sediment samples were collected from Thazhankuda (Cuddalore) to Kodiyakkarai of south east coast of Tamil Nadu, India. The study area is underlain by various geological formations ranging in age from oldest Archean to the Recent aluvium. In between there are semi-consolidated formed, which belong to Mesozoic and Tertiary ages. Detailed reviews about these rocks appear in the works on Cretaceous rocks of South India by Rao (1956) also appeared during the period. In the eastern part of the area, alluvial deposits of river Cauvery and its tributaries lie over the tertiary sandstone. They consist of medium to fine sands, gravelly sands, clays and sandy clays. The thickness of these formations ranges from 30 m in the inland to 40 m near the coasts. The northern part of the study area is covered with metamorphic crystalline rocks of Charnokite suite belonging to Archean age. Quaternary deposits are confined to the coastal area and floodplains of major rivers. The quaternary sediments are expected to result from the erosive action of various natural agents like winds, waves and rivers (Janardhanan 1986). The sediments consist of clay, silt and sand. The central coast of Tamil Nadu coastal tracks are divided into upland, floodplain, deltic plain and coastal plain (Loveson et al. 1990). Sandy beaches are seen

in narrow linear and discontinuous from the entire study area in tide dominated and a number of tidal creeks are there. The coast line is represented by undulating topography with a seaward slope.

### 2.2 Sampling and Sample Preparation

Sediment samples were collected along the Bay of Bengal coastline, from Thazhankuda (Cuddalore) to Kodiyakkarai coast during pre-monsoon condition. Table 1 represents the geographic latitude and longitude for the sampling locations in the study area. Sampling locations were selected to collect representative samples from all along the study area. Sediment sample was collected by a Peterson grab sampler from 5 m water depth parallel to the shoreline (Fig. 1). Then pebbles, leaves and other foreign particles were removed. The collected samples were air dried at room temperature in the open air, then brought to the laboratory, where they were dried for 12 h in an oven at 105 °C to constant mass. Sediment samples were sieved with a 250 micromesh laboratory test sieve. A volume of 100 cm<sup>3</sup> of each sample was then transferred to radon impermeable PVC cylindrical container of diameter 6.5 cm and height 7 cm. Containers were sealed tightly with vinyl tape around its screw neck to prevent possible escape of radon gases. Samples were then stored for a period of 4 weeks to allow radioactive equilibrium to be attained between <sup>238</sup>U (<sup>226</sup>Ra) and <sup>232</sup>Th (<sup>228</sup>Ra) and their progenies.

### 2.3 Gamma Spectrometric Analysis

All samples were subjected to gamma spectral analysis with a counting time of 10,000 s. A 3" × 3" NaI(Tl) detector was employed with adequate lead shielding which reduced the background by a factor of about 95%. The concentrations of various radionuclides of interest were determined in Bq kg<sup>-1</sup> using the count spectra. The certified reference materials supplied by International Atomic Energy Agency (IAEA) RGU-I, RGTh-I and RGK-I as standards in the same geometry and having the similar density, as that of the prepared sediment samples, were used for obtaining efficiency calibration of the detector for various energies in the prescribed geometry. Each reference standard was kept on the detector and respective spectrum was recorded and net counts in respective ROI were calculated.

#### 2.3.1 Calculation of Efficiency Factors

Net counts in each ROI is corrected for background and then the net cps in each ROI is arrive as given below

**Table 1** The geographical latitude and longitude for the sampling locations at the study area

S. no.	Sample ID	Latitude (N)	Longitude (E)	Location
1	CTK	11°46'7.06"	79°48'40.40"	Thazhankuda
2	CDM	11°43'46.84"	79°48'11.39"	Devanampattinum
3	COT	11°43'5.30"	79°48'11.73"	Singarrathoppu
4	CAP	11°35'11.38"	79°47'0.66"	Ayyampet
5	CSP	11°32'56.29"	79°46'48.59"	Samiyarpet
6	CPT	11°31'23.26"	79°47'15.73"	Parangipet
7	CPI	11°24'41.34"	79°50'13.01"	Pichavaram
8	KDM	11°22'53.02"	79°50'28.13"	Kodiyampalayam
9	NPZ	11°19'57.07"	79°51'2.77"	Pazhaiyar
10	NSI	11°13'48.86"	79°52'7.23"	Sirkazhi
11	NPB	11° 8'34.55"	79°52'42.17"	Poombukar
12	TRGB	11° 1'31.97"	79°52'53.12"	Tharangambadi
13	PKK	10°54'59.40"	79°52'12.23"	Karaikal
14	NGR	10°49'16.46"	79°52'21.05"	Nagore
15	NAP	10°44'42.24"	79°52'33.60"	Akkaraipettai
16	VLK	10°41'2.93"	79°52'35.61"	Velankanni
17	TPI	10°37'39.79"	79°52'49.71"	Thirupoondi
18	VKT	10°33'16.64"	79°53'15.85"	Vettaikaranthoppu
19	VED	10°22'58.20"	79°55'37.80"	Vedaranium
20	KODI	10°19'55.85"	79°58'1.53"	Kodiyakkarai

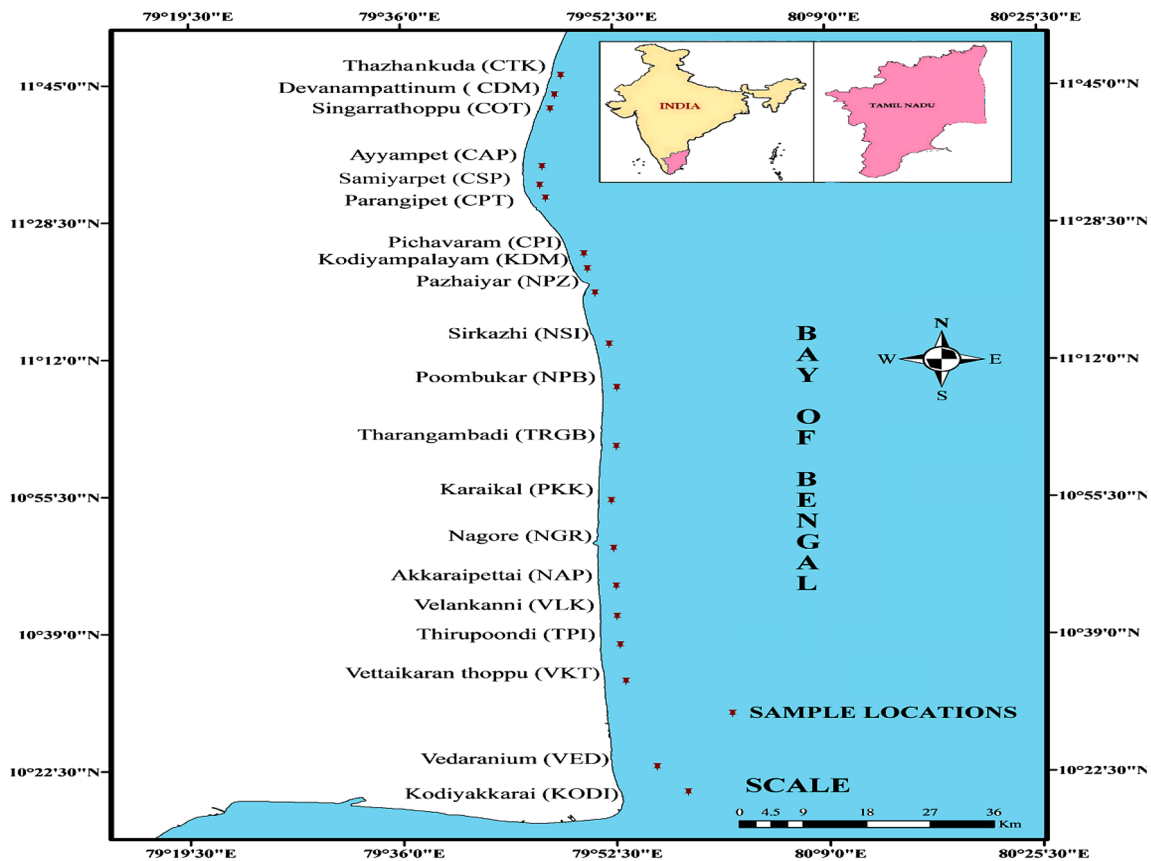


**Fig. 1** Location map

**Table 2** Radiological parameters in coastal sediment samples of East Coast line of study area

S. no.	Sample ID	Activity concentration (Bq kg <sup>-1</sup> ) <sup>238</sup> U <sup>232</sup> Th <sup>40</sup> K	R <sub>eq</sub> (Bq kg <sup>-1</sup> )	Absorbed dose rate (D <sub>R</sub> ) (nGy h <sup>-1</sup> )	Annual effective dose rate (AEDE) (mSv year <sup>-1</sup> )	AGDE (mSv year <sup>-1</sup> )	Activity utilization index (AUI)	H <sub>ex</sub>	H <sub>in</sub>	Gamma index (Γ <sub>r</sub> )	ELCR × 10 <sup>-3</sup>	Radioactive heat production (RHP) rate (μWm <sup>-3</sup> )
1	CTK	BDL 43.74 375.18	91.44	42.18	0.052	0.301	0.560	0.247	0.247	0.688	0.182	0.5914
2	CDM	BDL 21.74 374.11	59.89	28.84	0.035	0.208	0.294	0.162	0.162	0.467	0.124	0.3528
3	COT	BDL 21.98 383.56	60.97	29.39	0.036	0.212	0.298	0.165	0.165	0.476	0.127	0.3617
4	CAP	BDL 6.48 341.72	35.58	18.27	0.022	0.134	0.107	0.096	0.096	0.293	0.079	0.1820
5	CSP	BDL BDL 352.7	27.16	14.81	0.018	0.111	0.029	0.073	0.073	0.235	0.064	0.1353
6	CPT	BDL BDL 338.95	26.10	14.24	0.018	0.106	0.028	0.070	0.070	0.226	0.061	0.1351
7	CPI	9.95 71.33 299.71	135.03	60.27	0.074	0.423	0.979	0.365	0.391	0.979	0.259	1.0739
8	KDM	BDL 5.36 383	37.16	19.32	0.024	0.143	0.097	0.100	0.100	0.309	0.083	0.1876
9	NPZ	BDL BDL 410.9	31.64	17.26	0.021	0.129	0.034	0.085	0.085	0.274	0.074	0.1575
10	NSI	10.71 17.63 400.81	66.78	32.43	0.040	0.232	0.345	0.180	0.209	0.515	0.140	0.4508
11	NPB	BDL 9.03 429.56	45.99	23.50	0.029	0.173	0.145	0.124	0.124	0.377	0.101	0.2387
12	TRGB	BDL 38.59 376.77	84.19	39.13	0.048	0.280	0.498	0.227	0.227	0.637	0.168	0.5664
13	PKK	45.31 472.75 384.36	750.94	322.62	0.397	2.237	6.162	2.028	2.150	5.286	1.389	6.7310
14	NGR	BDL 22.63 408.24	63.80	30.81	0.038	0.223	0.307	0.172	0.172	0.498	0.133	0.3790
15	NAP	BDL 15.06 325.29	46.58	22.76	0.028	0.165	0.209	0.126	0.126	0.367	0.098	0.2904
16	VLK	BDL 24.98 388.89	65.67	31.42	0.039	0.227	0.334	0.177	0.177	0.509	0.135	0.4092
17	TPI	BDL 20.4 342.44	55.54	26.70	0.033	0.193	0.275	0.150	0.150	0.432	0.115	0.3609
18	VKT	BDL 8.7 512.64	51.91	26.79	0.033	0.197	0.148	0.140	0.140	0.429	0.115	0.2277
19	VED	BDL 8.52 488.82	49.82	25.68	0.032	0.189	0.144	0.135	0.135	0.411	0.111	0.2233
20	KODI	BDL BDL 467.91	36.03	19.65	0.024	0.147	0.039	0.097	0.097	0.312	0.085	0.1514
	Average	3.3 40.45 389.28	91.11	42.30	0.052	0.301	0.552	0.246	0.255	0.686	0.182	0.6603

$$\text{Net CPS in ROI} = \frac{\text{Grosscounts in ROI} - \text{Gross BKG counts in ROI}}{\text{Counting time (s)}}$$

Then the efficiency factor “ $\eta$ ” for that energy ROI is calculated using the formula

$$\text{Efficiency factor } (\eta) = \frac{\text{Net CPS in ROI}}{\text{Activity (Bq)}}$$

The radionuclide, activity, the gamma energy used, ROI, background counts, standard counts are calculated.

The gamma-ray photo peaks corresponding to 1.46 MeV ( $^{40}\text{K}$ ), 1.76 MeV ( $^{214}\text{Bi}$ ) and 2.614 MeV ( $^{208}\text{Tl}$ ) were considered in arriving at the activity of  $^{40}\text{K}$ ,  $^{238}\text{U}$  and  $^{232}\text{Th}$  in the samples. The detection limit of NaI(Tl) detector system for  $^{40}\text{K}$ ,  $^{238}\text{U}$  and  $^{232}\text{Th}$  are 8.5, 2.21 and 2.11 Bq kg<sup>-1</sup>, respectively, for a counting time of 10,000 s.

The activity content (Bq/kg) in each sample is estimated as given below:

$$\text{Net CPS in ROI} = \frac{\text{Net counts in ROI} - \text{Net BKG counts in ROI}}{\text{Counting time (s)}}$$

$$\text{Activity (Bq/kg)} = \frac{\text{Net CPS in ROI}}{\eta \times \text{Sample wt (kg)}}$$

where ‘ $\eta$ ’ is the efficiency factor (cps/Bq) of correspond energy ROI.

### 3 Results and Discussions

#### 3.1 Activity Concentrations of $^{238}\text{U}$ , $^{232}\text{Th}$ and $^{40}\text{K}$ in the Sediments

The results of analysis of activity concentration  $^{238}\text{U}$ ,  $^{232}\text{Th}$  and  $^{40}\text{K}$  radionuclides in beach sediment samples for different locations of the study area are presented in Table 2. Activity is

reported in Bq kg<sup>-1</sup> on the basis of the sediment’s dry weight. The activity concentrations range and mean values (in properties brackets) of the activities for  $^{238}\text{U}$ ,  $^{232}\text{Th}$  and  $^{40}\text{K}$  are  $\leq 2.21\text{--}45.31$  (3.30),  $\leq 2.11\text{--}472.75$  (40.45) and 299.71–512.64 (389.28) Bq kg<sup>-1</sup>, respectively. Measured activities of the radionuclides differed widely, as activity levels in the marine environment depend on their physical, chemical and geochemical and the environment (de Mora et al. 2004).

From the results it is clear that the mean activity of  $^{238}\text{U}$  and  $^{40}\text{K}$  are lower while  $^{232}\text{Th}$  is greater when compared with worldwide average value as shown in Table 3. The concentration of activity levels in Karaikal is greater than the worldwide average values. Table 4 provides the comparison of activity concentration within India. Figure 2 shows the variation of activity concentration at different sampling locations. The average values of activity do not provide an exact indication of radiation hazard associated with the materials.

#### 3.2 Radium Equivalent Activity

Radium equivalent index in Bq kg<sup>-1</sup> is a widely used radiological hazard index which is calculated using the formula given by Beretka and Matthew (1985)

$$\text{Ra}_{\text{eq}} = A_{\text{U}} + 1.43A_{\text{Th}} + 0.077A_{\text{K}}, \tag{1}$$

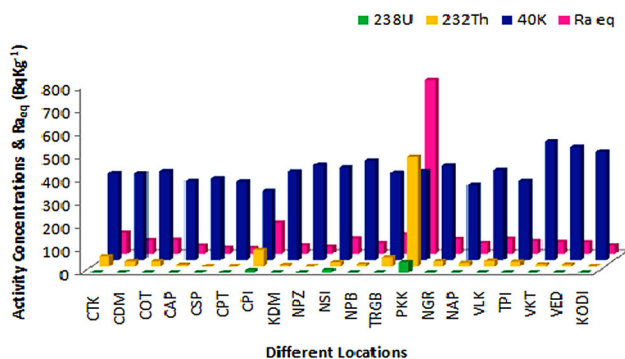
where  $A_{\text{U}}$ ,  $A_{\text{Th}}$  and  $A_{\text{K}}$  are the specific activities of  $^{238}\text{U}$ ,  $^{232}\text{Th}$  and  $^{40}\text{K}$  (Bq kg<sup>-1</sup>), respectively. The radium equivalent activity ( $\text{Ra}_{\text{eq}}$ ) in these sediment samples ranges from 26.10 to 750.94 Bq kg<sup>-1</sup> with a mean value of 91.11 Bq kg<sup>-1</sup> (Table 2) which is less (four times) than the recommended maximum value of 370 Bq kg<sup>-1</sup> (Beretka and Matthew 1985). This high value (750.94 Bq kg<sup>-1</sup>) noticed at PKK due to high concentration of uranium and thorium in sediment samples. Figure 2 shows the locations and radium equivalent activity ( $\text{Ra}_{\text{eq}}$ ).

**Table 3** Worldwide average value

Parameters	World average	References
Concentration of $^{238}\text{U}$ (Bq kg <sup>-1</sup> )	35	UNSCEAR (2000)
Concentration of $^{232}\text{Th}$ (Bq kg <sup>-1</sup> )	30	UNSCEAR (2000)
Concentration of $^{40}\text{K}$ (Bq kg <sup>-1</sup> )	400	UNSCEAR (2000)
$\text{Ra}_{\text{eq}}$ (Bq kg <sup>-1</sup> )	370	Beretka and Matthew (1985); NEA-OECD (1979)
$D_{\text{R}}$ (nGyh <sup>-1</sup> )	84	UNSCEAR (2000)
AEDE (mSv year <sup>-1</sup> )	0.46	UNSCEAR (1993)
$H_{\text{ex}}$	1	ICRP 60 (1990)
$H_{\text{in}}$	1	ICRP 60 (1990)
$I_{\text{yr}}$	1	UNSCEAR (2000)
$\text{ELCR} \times 10^{-3}$	0.29	UNSCEAR (2000)

**Table 4** Comparison of activity concentration of present work within India

S. no.	Name of the location	Activity concentration (Bq kg <sup>-1</sup> )			References
		<sup>238</sup> U	<sup>232</sup> Th	<sup>40</sup> K	
1	East coast of Tamil Nadu (coastal sediment)	BDL	14.29	360.23	Ravisankar et al. (2015)
2	NE Coast, Tamil Nadu, India	35.12	713.6	349.6	Sureshgandhi et al. (2014)
3	NE Coast, Tamil Nadu, India	8	25	275	Ramasamy et al. (2009)
4	Orissa, India	350	2000	200	Sengupta et al. (2005)
5	Eastern Orissa, India	350	2825	180	Mohanty et al. (2004)
6	Kalpakkam, Tamil Nadu, India	112	1456	351	Kannan et al. (2002)
7	Coastal Karnataka of South India	61–316.7	20.1–62.3	14.3–48.6	Narayana et al. (2001)
8	Ullal, Karnataka, India	374	158	158	Radhakrishna et al. (1993)
9	Visakhapatnam, India	–	100–400	300–600	Kalyani et al. (1990)
10	India	28.67	63.83	327.6	UNSCEAR (2000)
11	India (East Coast of Tamil Nadu)	3.30	40.45	389.28	Present work

**Fig. 2** Locations vs. activity concentration and radium equivalent activity (Bq kg<sup>-1</sup>)

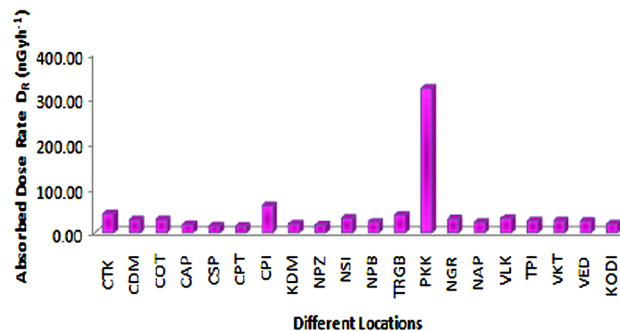
## 4 Evaluation of Radiological Hazard Effects

### 4.1 Absorbed Gamma Dose Rate ( $D_R$ )

The external gamma absorbed dose rate due to terrestrial  $\gamma$ -rays in air (nGy h<sup>-1</sup>) at 1 m above the ground level was calculated using formula given by UNSCEAR (2000). The dose conversion factors for converting the activity concentrations of <sup>238</sup>U, <sup>232</sup>Th and <sup>40</sup>K into dose rates (nGy h<sup>-1</sup> per Bq kg<sup>-1</sup>) are 0.462, 0.604 and 0.042 respectively.

$$D_R (\text{nGy h}^{-1}) = 0.462C_U + 0.604C_{Th} + 0.042C_K, \quad (2)$$

where  $C_U$ ,  $C_{Th}$  and  $C_K$  are the activity concentration of <sup>238</sup>U, <sup>232</sup>Th and <sup>40</sup>K in (Bq kg<sup>-1</sup>), respectively. From Table 2, it is clear that all the absorbed dose rate values in the studied area are lower than the world average of 84 nGy h<sup>-1</sup> (UNSCEAR 2000) except Karaikal which is 3.84 times greater than the world average value. This is due to high value for <sup>232</sup>Th activity concentration and could be explained by the presence of black sands, which are enriched in the mineral monazite containing a significant

**Fig. 3** Locations vs. absorbed gamma dose rate (nGy h<sup>-1</sup>)

amount of <sup>232</sup>Th (Ravisankar et al. 2015). The enrichment occurs because the specific gravity of monazite allows its concentration along beaches where lighter materials are swept away (Uosif et al. 2008). Figure 3 shows the variation of the absorbed gamma dose rate in different locations.

### 4.2 Annual Effective Dose Equivalent (AEDE)

The annual effective dose equivalent (AEDE) should be obtained to test the health effect of those absorbed dose rates. To estimate the annual effective doses, one has to take into account to conversion coefficient from absorbed dose in air to effective and the outdoor occupancy factor. In the UNSCEAR (2000) reports, a value of 0.7 SvGy<sup>-1</sup> was used for the conversion coefficient from the absorbed dose in air to the effective dose received by adults and the outdoor occupancy factor (0.2) which implies that people spend 20% of the time outdoors, on the average, around the world. The annual effective dose equivalent in mSv year<sup>-1</sup> resulting from the absorbed dose values ( $D_R$ ) was calculated using the following formula UNSCEAR (2000).



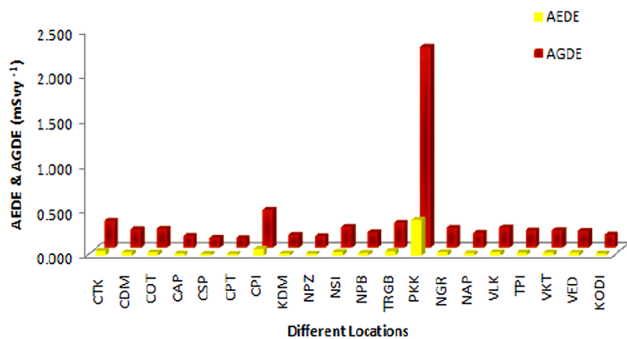


**Fig. 4** Locations vs. annual effective dose equivalent and AGDE ( $\text{mSv year}^{-1}$ )

$$AEDE = D_R (\text{nGy h}^{-1}) \times 8760 \text{ h} \times 0.2 \times 0.7 \text{ Sv Gy}^{-1} \times 10^{-6}$$

$$AEDE (\text{mSv year}^{-1}) = D_R \times 0.00123. \tag{3}$$

The annual effective dose equivalent obtained (Table 2) ranged between 0.018 and 0.397 with a mean value of  $0.052 \text{ mSv year}^{-1}$ . In areas with the normal background radiation, the average annual external effective dose from terrestrial radionuclides is  $0.46 \text{ mSv year}^{-1}$  (UNSCEAR 1993). Therefore, the obtained mean value from this study area ( $0.052 \text{ mSv year}^{-1}$ ) is lower than the world average value. Figure 4 shows the variation of annual effective dose equivalent in different locations.

### 4.3 Annual Gonadal Dose Equivalent (AGDE)

It is a measure of the genetic significance of the yearly dose equivalent received by the population’s reproductive organs (gonads). In the same context, the activity bone marrow and the bone surface cells are considered as the organs of interest by UNSCEAR (1988). Therefore, the annual gonadal dose equivalent (AGDE) due to the specific activities of  $^{238}\text{U}$ ,  $^{232}\text{Th}$  and  $^{40}\text{K}$  were calculated using the following formula (Ravisankar et al. 2014; Sivakumar et al. 2014):

$$AGDE (\mu\text{Sv year}^{-1}) = 3.09A_U + 4.18A_{Th} + 0.314A_K. \tag{4}$$

The AGDE values are presented in Table 2. The overall average value of AGDE is found to be  $301.49 \mu\text{Sv year}^{-1}$ . As can be seen, the average values do not, in general, exceed the permissible recommended limits, indicating that the hazardous effects of these radiations are negligible. But, it exceeds in Karaikal location. Figure 4 shows the locations and annual gonadal dose equivalent (AGDE).

### 4.4 Activity Utilization Index (AUI)

To facilitate the calculation of dose rates in air from different combinations of the three radionuclides in sediments and by applying the appropriate conversion factors, an activity utilization index (AUI) is constructed that is given

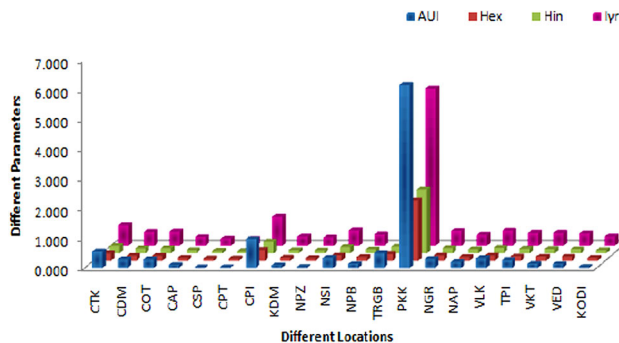


**Fig. 5** Locations vs. different parameters (AUI,  $H_{ex}$ ,  $H_{in}$  and  $I_{yr}$ )

by the following formula (El-Gamal et al. 2007; Ravisankar et al. 2014; Sivakumar et al. 2014):

$$AUI = \left( \frac{A_U}{50 \text{ Bq/kg}} \right) f_U + \left( \frac{A_{Th}}{50 \text{ Bq/kg}} \right) f_{Th} + \left( \frac{A_K}{500 \text{ Bq/kg}} \right) f_K, \tag{5}$$

where  $A_U$ ,  $A_{Th}$  and  $A_K$  are the activity concentrations (in  $\text{Bq kg}^{-1}$ ) of  $^{238}\text{U}$ ,  $^{232}\text{Th}$  and  $^{40}\text{K}$  and  $f_U$ ,  $f_{Th}$  and  $f_K$  are the fractional contributions to the total dose rate in air due to gamma radiation from the actual concentrations of these radionuclides. In the NEA-OECD (1979) Report, typical activities per unit mass of  $^{238}\text{U}$ ,  $^{232}\text{Th}$  and  $^{40}\text{K}$  in sediments  $A_U$ ,  $A_{Th}$  and  $A_K$  are referred to be 50, 50 and  $500 \text{ Bq kg}^{-1}$ , respectively. The activity utilization index of the sediment samples are calculated using the above formula. The calculated values (Table 2) vary from 0.028 to 6.162 with an average of 0.552. This value shows that AUI is less than 2 (except Karaikal) for 19 locations, which corresponds to an annual effective dose  $<0.3 \text{ mSv year}^{-1}$  (El-Gamal et al. 2007). This indicates that these sediments can be safely used for construction. Figure 5 shows the locations and activity utilization index (AUI).

## 5 Radiation Hazard Indices

### 5.1 External Hazard Index ( $H_{ex}$ )

The external hazard index ( $H_{ex}$ ) represents the external radiation exposure associated with gamma radiation from radionuclides of concern. The value of  $H_{ex}$  should not exceed the maximum acceptable value of  $1 \text{ mSv year}^{-1}$  to keep the hazard insignificant (ICRP 60 1990). This index can be evaluated using the following equation,

$$H_{ex} = \frac{A_U}{370 \text{ Bq/Kg}} + \frac{A_{Th}}{259 \text{ Bq/Kg}} + \frac{A_K}{4810 \text{ Bq/Kg}}. \tag{6}$$

The maximum value of unity for  $H_{ex}$  corresponds to the limit of  $370 \text{ Bq kg}^{-1}$  for  $Ra_{eq}$ . The calculated value of the external hazard index for the studied samples is presented in Table 2. The  $H_{ex}$  values ranged from 0.07 to 2.028 with an average value of 0.246, so the samples meet the condition  $H_{ex} < 1$ . This implies that activities involving the use of sediment samples are safe and do not attract any high levels of radiation exposure. Figure 5 shows the locations and  $H_{ex}$ .

## 5.2 Internal Hazard Index ( $H_{in}$ )

The internal hazard index ( $H_{in}$ ) is used to control the internal exposure to  $^{222}\text{Rn}$  and its radioactive progeny (Al-Trabulsy et al. 2011). The internal exposure to radon and its daughter products is quantified by the internal hazard index ( $H_{in}$ ), which is given by the following equation (Krieger 1981).

$$H_{in} = \frac{A_U}{185 \text{ Bq/kg}} + \frac{A_{Th}}{259 \text{ Bq/kg}} + \frac{A_K}{4810 \text{ Bq/kg}}. \quad (7)$$

The average value of  $H_{in}$  has been determined to be 0.255 (Table 2) which is also less than one which indicates that the internal hazards are less than the critical value. Figure 5 shows the locations and  $H_{in}$ .

## 6 Gamma Representative Level Index ( $I_{\gamma r}$ )

An additional hazard index so-called representative level index is calculated by using the formula (NEA-OECD 1979; Harb 2008):

$$I_{\gamma r} = \frac{A_U}{150} + \frac{A_{Th}}{100} + \frac{A_K}{1500}. \quad (8)$$

This index can be used to estimate the level of  $\gamma$ -radiation hazard associated with the natural radionuclides, where  $A_U$ ,  $A_{Th}$  and  $A_K$  are the specific activities of  $^{238}\text{U}$ ,  $^{232}\text{Th}$  and  $^{40}\text{K}$  ( $\text{Bq kg}^{-1}$ ), respectively. Table 2 represents the values for the representative index ranged between 0.226 and 5.286 with a mean value of 0.686. Values of  $I_{\gamma r} \leq 1$  correspond to an annual effective dose of less than or equal to 1 mSv. No exceeding of the recommended upper limit is noted in 19 locations, except Karaikal which is 5.2 times the world average value (Unity). This exceedance in this site is due to the high concentration of radionuclides. Figure 5 shows the locations and gamma representative level index ( $I_{\gamma r}$ ).

## 7 Excess Lifetime Cancer Risk (ELCR)

Excess lifetime cancer risk (ELCR) is calculated using the following equation (Taskin et al. 2009) and presented in Table 2.

$$\text{ELCR} = \text{AEDE} \times \text{DL} \times \text{RF}, \quad (9)$$

where AEDE, DL and RF are the total annual effective dose equivalent, duration of life (70 years) and risk factor ( $\text{Sv}^{-1}$ ), i.e. fatal cancer risk per sievert, respectively. For stochastic effects, ICRP 60 (1990) uses values of 0.05 for the public (Taskin et al. 2009). The ELCR values were found to be higher in Karaikal (Table 2). This may be due to the higher activity concentration in the sampling locations. From Table 2, the calculated ELCR values ranged from  $0.061 \times 10^{-3}$  to  $1.389 \times 10^{-3}$  with an average of  $0.182 \times 10^{-3}$ , which is lower than the worldwide recommended value of  $0.29 \times 10^{-3}$  (UNSCEAR 2000). Figure 6 shows the locations and excess lifetime cancer risk (ELCR).

## 8 Radioactive Heat Production (RHP) Rate

Radioactive elements found in the crust and mantle form the basis for several major applications in geophysics and geochemistry. The heat produced by naturally occurring elements is a key factor in geothermal studies, especially in the interpretation of continental heat-flow density data. The major internal heat source of the earth is the subject of several studies due to its importance in modeling the thermal evaluation of the lithosphere. The radioactive isotopes  $^{238}\text{U}$ ,  $^{232}\text{Th}$  and  $^{40}\text{K}$  contribute most of the terrestrial heat flow. These elements are fundamental for understanding the nature of the mantle, crust of the earth and their heat generating potential. The radioactive heat production ( $A$ ) rate of sediments (RHP in  $\mu\text{Wm}^{-3}$ ) can be calculated by taking into account the heat generation constant (amount of heat released per gram U, Th and K per unit time) and from the uranium, thorium and potassium concentrations  $C_U$ ,  $C_{Th}$ ,  $C_K$  (Rybach 1988; Cermak et al. 1982).

$$A = 10^{-5} \rho (9.52C_U + 2.56C_{Th} + 3.48C_K) \mu\text{Wm}^{-3}, \quad (10)$$

where  $\rho$  is the sample density (in  $\text{kg m}^{-3}$ );  $C_U$  and  $C_{Th}$  are activity concentration of uranium and thorium in weight ppm;  $C_K$  is activity concentration of potassium in weight

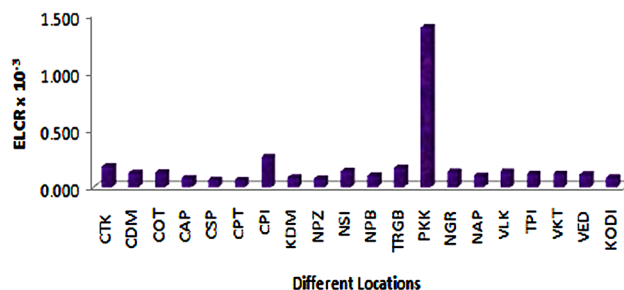


Fig. 6 Locations vs. ELCR



%. The activity concentration of radionuclides ( $\text{Bq kg}^{-1}$ ) is converted into ppm and % using conversion factors quoted by Mohanty et al. (2004). In the present study, the heat production rate ranges from 0.1351 to 6.7310  $\mu\text{Wm}^{-3}$  with a mean value of 0.6603  $\mu\text{Wm}^{-3}$ . All the locations showed low RHP rate (below 1  $\mu\text{Wm}^{-3}$ ) except Karaikal (PKK) location (Table 2). This highest value of RHP rate in Karaikal (PKK) may be due to the presence of increased content of the radioactive thorium  $^{232}\text{Th}$  and increased amounts of accessory minerals (Helbig and Treitel 1996). From the analysis, more dense measurements are necessary for further investigation of radiogenic heat production in the study area.

## 9 Multivariate Statistical Analysis

The multivariate statistical analysis, such as correlation, principal component and cluster analysis were performed using the radioactive variables to know the existing relation between them. The statistical software SPSS (16.0 version) was used to elucidate the relationships between radioactive variables. The correlation between coefficient is significant with  $p$  value  $<0.05$  (Chandrasekaran et al. 2015).

### 9.1 Descriptive Statistics of Radionuclides

The Basic statistics such as minimum, maximum, mean, standard deviation, variance, skewness and kurtosis were used to describe the statistical characteristics of the radionuclide activities and the results are presented in Table 5.

The standard deviation higher than the mean value indicates the low degree of uniformity and vice versa (Ravisankar et al. 2014). In the present study, standard deviation of  $^{238}\text{U}$  and  $^{232}\text{Th}$  are greater than their mean value. This shows that the concentration of uranium and thorium in sediment samples has a low degree of uniformity. The standard deviation of  $^{40}\text{K}$  is less than the mean value which indicates a high degree of uniformity in their

**Table 5** Descriptive statistical characteristics of radioactive variables

Variables	$^{238}\text{U}$	$^{232}\text{Th}$	$^{40}\text{K}$
Mean	3.29	40.44	389.27
Std. Deviation	10.38	103.26	53.81
Variance	107.84	10,663.76	2895.65
Skewness	3.87	4.26	0.77
Kurtosis	15.85	18.66	0.51
Minimum	BDL	BDL	299.71
Maximum	45.31	472.75	512.64

distribution. The skewness of the data set indicates whether deviations from the mean are likely to be positive or negative. Positive skewness indicates a distribution with an asymmetric tail extending towards values that are more positive. Negative skewness indicates a distribution with an asymmetric tail extending towards values that are more negative. Lower skewness values indicate generally normal distributions. The activity concentrations of all the radionuclides in this study have positive skewness values (Table 5), which indicate that the distributions are asymmetric in nature. Kurtosis is a measure of the peakedness of the probability distribution of a real-valued random variable. Positive kurtosis indicates a relatively peaked distribution. Negative kurtosis indicates a relatively flat distribution. Higher kurtosis means that more of the variance is the result of infrequent extreme deviations, as opposed to frequent modestly sized deviations. In the present case, the distributions associated with all the radionuclides have positive kurtosis values (Table 5), indicating peaked distributions.

The frequency distributions of all the radionuclides were analyzed, and the histograms are given in Figs. 7, 8 and 9, for  $^{40}\text{K}$  shows that these radionuclides demonstrate a normal (bell-shaped) distribution. However,  $^{238}\text{U}$  and  $^{232}\text{Th}$  exhibit some degree of multi-modality. This multi-modal feature of the radioactive elements demonstrates the complexity of minerals in building materials.

### 9.2 Correlation Analysis

Correlation analysis was carried out to determine the mutual relations and strengths of association between pairs of variables through the calculation of the Pearson correlation coefficients. The results for the Pearson correlation coefficients between all the radioactive variables given in Table 6.

A high-positive correlation coefficient is observed between  $^{232}\text{Th}$  and  $^{238}\text{U}$  because the uranium and thorium

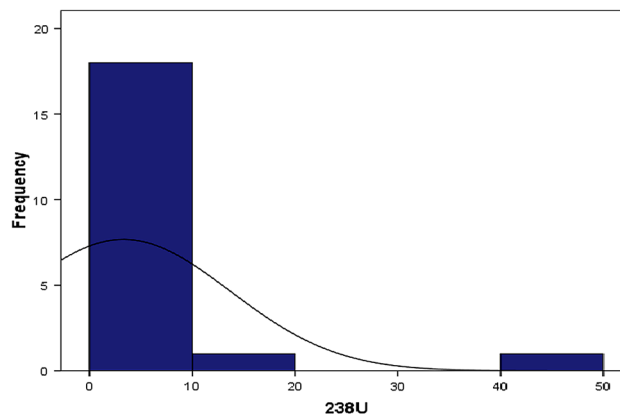


**Fig. 7** Frequency distribution of  $^{238}\text{U}$

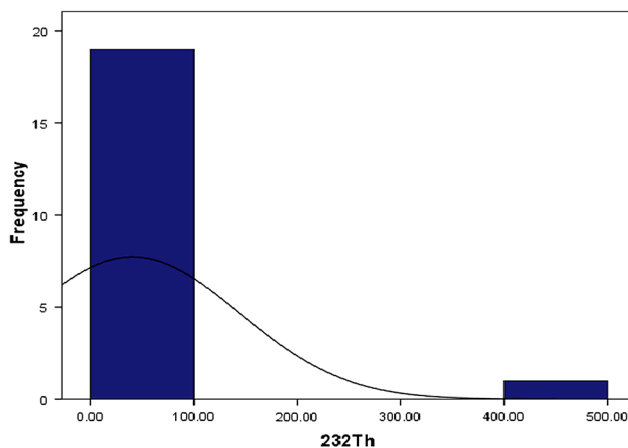


Fig. 8 Frequency distribution of  $^{232}\text{Th}$

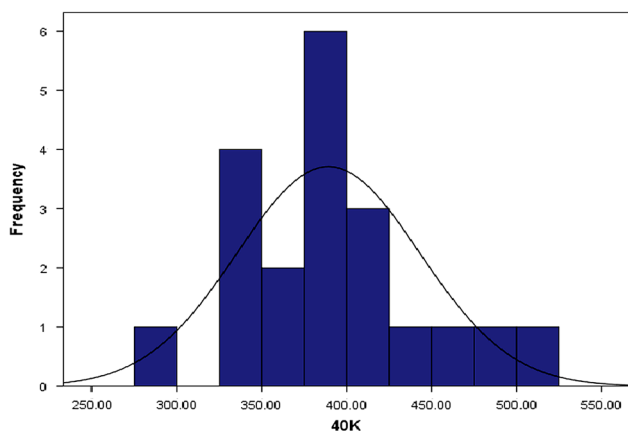


Fig. 9 Frequency distribution of  $^{40}\text{K}$

decay series occur together in nature (Tanaskovic et al. 2012). In contrast, a very weak negative correlation coefficient is observed between these two nuclides and  $^{40}\text{K}$

because  $^{40}\text{K}$  is of different origin. In addition, all radioactive variables have strong positive correlation coefficients with  $^{238}\text{U}$  and  $^{232}\text{Th}$ , while they are weakly negatively correlated with  $^{40}\text{K}$ . All the radiological parameters are existing due to concentration of  $^{238}\text{U}$  and  $^{232}\text{Th}$  whereas  $^{40}\text{K}$  is not contributing to radioactivity.

### 9.3 Principal Component Analysis

Using principal component analysis (PCA) radioactive variables are linearly combined, and new fundamental components that can provide a better description and a quantitative interpretation of geochemical data (Chandrasekaran et al. 2015).

Principal component analysis was carried out between 12 radioactive variables. The rotated factor analysis was performed via varimax rotation with Kaiser normalization. The rotated component 1 and component 2 values are reported in Table 7. The principal component analysis yielded two components with eigenvalues  $>1$ , explaining 99.46% of the total variance. From the rotation space of component 1 and component 2 (Fig. 10), the first component accounts for 91.01% of the total variance and is mainly characterized by high positive loading of concentrations of  $^{232}\text{Th}$  and  $^{238}\text{U}$ . Component 2 accounts for 8.45% of the total variance and mainly corresponds to positive loading of  $^{40}\text{K}$ . From the overall factor analysis, it can be deduced that  $^{232}\text{Th}$  and  $^{238}\text{U}$  increase the radioactivity. The results of PCA good agreement with correlation analysis.

### 9.4 Cluster Analysis

Cluster analysis is a data classification technique that comprises a series of multivariate methods, which are used

Table 6 Pearson correlation coefficients between the radioactive variables

Variables	$^{238}\text{U}$	$^{232}\text{Th}$	$^{40}\text{K}$	$\text{Ra}_{\text{eq}}$	DR	AEDR	AGDE	AUI	$H_{\text{ex}}$	$H_{\text{in}}$	$I_{\gamma\text{r}}$	ELCR
$^{238}\text{U}$	1											
$^{232}\text{Th}$	0.964	1										
$^{40}\text{K}$	-0.093	-0.091	1									
$\text{Ra}_{\text{eq}}$	0.968	1.000	-0.065	1								
DR	0.969	0.999	-0.058	1.000	1							
AEDR	0.969	0.999	-0.057	1.000	1.000	1						
AGDE	0.968	0.999	-0.055	1.000	1.000	1.000	1					
AUI	0.969	1.000	-0.088	1.000	1.000	1.000	0.999	1				
$H_{\text{ex}}$	0.968	1.000	-0.065	1.000	1.000	1.000	1.000	1.000	1			
$H_{\text{in}}$	0.972	0.999	-0.067	1.000	1.000	1.000	1.000	1.000	1.000	1		
$I_{\gamma\text{r}}$	0.968	0.999	-0.059	1.000	1.000	1.000	1.000	1.000	1.000	1.000	1	
ELCR	0.969	0.999	-0.058	1.000	1.000	1.000	1.000	1.000	1.000	1.000	1.000	1

**Table 7** Rotated factor loadings of radioactive variables

Variables	Component-1	Component-2
$^{238}\text{U}$	0.9661	-0.0598
$^{232}\text{Th}$	0.9983	-0.0568
$^{40}\text{K}$	-0.0345	0.9994
$\text{Ra}_{\text{eq}}$	0.9995	-0.0309
DR	0.9997	-0.0235
AEDR	0.9997	-0.0228
AGDE	0.9998	-0.0207
AUI	0.9985	-0.0538
$H_{\text{ex}}$	0.9995	-0.0310
$H_{\text{in}}$	0.9993	-0.0327
$I_{\gamma\text{r}}$	0.9997	-0.0245
ELCR	0.9997	-0.0233
% of variance explained	91.01	8.45

to find true groups of data (Ravisankar et al. 2014). In cluster analysis, observations with the largest similarity are grouped first, and then the next most similar observations are grouped successively. The grouping of the variables is usually represented as dendrogram. The derived dendrogram is shown in Fig. 11.

All the clusters are formed on the basis of existing similarities. In this dendrogram, all 12 variables are grouped into two statistically significant clusters. Cluster 1 consists of  $^{238}\text{U}$ ,  $^{232}\text{Th}$ ,  $\text{Ra}_{\text{eq}}$ , DR, AEDR, AGDE, AUI,  $H_{\text{ex}}$ ,  $H_{\text{in}}$ ,  $I_{\gamma\text{r}}$  and ELCR. This shows that the total level of

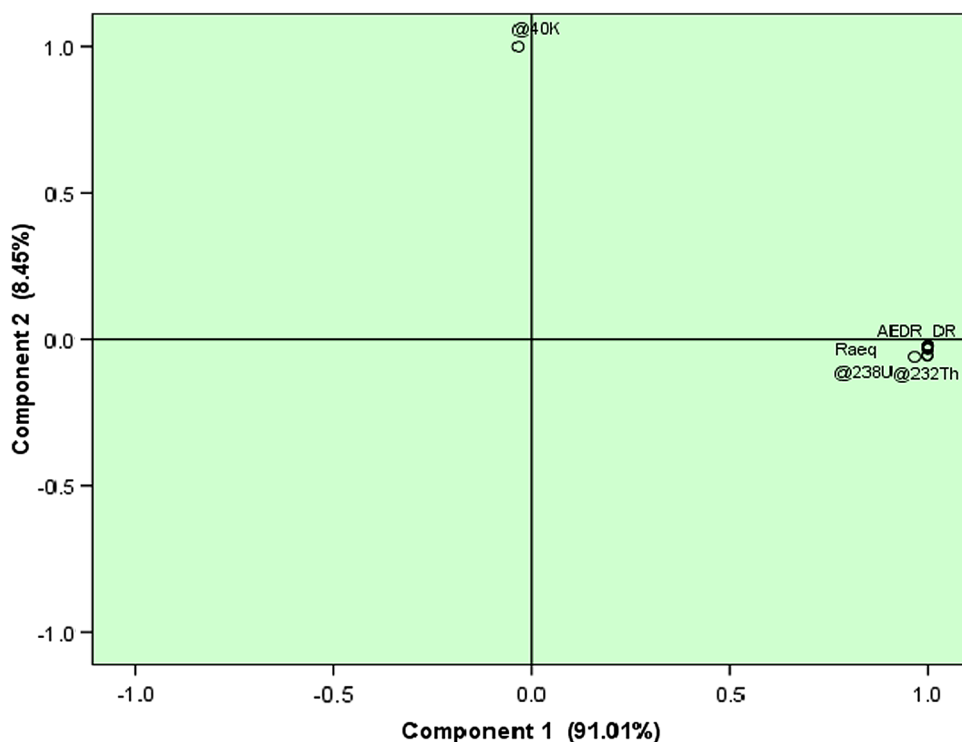
radioactivity in sediment mainly depends on the corresponding  $^{238}\text{U}$  and  $^{232}\text{Th}$  concentrations. Similarly cluster 2 consists of only  $^{40}\text{K}$  suggesting that the concentration of potassium in sediments not contributing the radiation hazard in the sediment sampling locations. These results are in good agreement with Pearson correlation and principal component analysis.

### 9.5 Activity Ratio

$^{238}\text{U}$  and  $^{232}\text{Th}$  commonly occur together in nature. This is frequently leads to a relatively constant  $^{238}\text{U}/^{232}\text{Th}$  ratio in many natural systems. This ratio may vary from the original value if the sample was subjected to physical or chemical interactions that may affect one series more or less than the other one. The distribution of uranium, thorium and potassium was disequilibrium in sediment samples. To know the distribution status of uranium, thorium and potassium, spatial distribution of radionuclides is studied.

The calculated  $^{238}\text{U}/^{232}\text{Th}$ ,  $^{232}\text{Th}/^{238}\text{U}$ ,  $^{232}\text{Th}/^{40}\text{K}$  and  $^{238}\text{U}/^{40}\text{K}$  ratios are given in Table 8. The ratio of  $^{238}\text{U}/^{232}\text{Th}$  is varied from 0.05 to 0.64 with an average of 0.36.  $^{232}\text{Th}/^{238}\text{U}$  ranged from 0.95 to 19.79 with an average value of 6.75.  $^{232}\text{Th}/^{40}\text{K}$  ranged from 0.01 to 1.23 with an average value of 0.11.  $^{238}\text{U}/^{40}\text{K}$  varied in the range of 0.01 to 0.12 with an average value of 0.01. This ratio can be used as an indicator of the relative occurrence of these radionuclides. Figure 12 shows the spatial distribution of radionuclides. It was noticed that  $^{232}\text{Th}$  activity

**Fig. 10** Rotated factor loadings of component-1 (91.01%) and component-2 (8.45%)



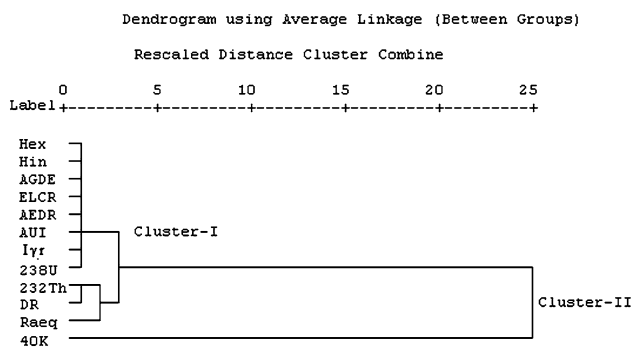


**Fig. 11** Dendrogram shows the clustering of radionuclides

**Table 8** Activity ratios

S.No.	Sample ID	$^{238}\text{U}/^{232}\text{Th}$	$^{232}\text{Th}/^{238}\text{U}$	$^{232}\text{Th}/^{40}\text{K}$	$^{238}\text{U}/^{40}\text{K}$
1	CTK	0.05	19.79	0.12	0.01
2	CDM	0.10	9.84	0.06	0.01
3	COT	0.10	9.95	0.06	0.01
4	CAP	0.04	2.93	0.02	0.01
5	CSP	0.05	0.95	0.01	0.01
6	CPT	0.05	0.95	0.01	0.01
7	CPI	0.14	7.17	0.24	0.03
8	KDM	0.01	2.43	0.01	0.01
9	NPZ	0.05	0.95	0.01	0.01
10	NSI	0.61	1.65	0.04	0.03
11	NPB	0.24	4.09	0.02	0.01
12	TRGB	0.06	17.46	0.10	0.01
13	PKK	0.10	10.43	1.23	0.12
14	NGR	0.10	10.24	0.06	0.01
15	NAP	0.15	6.81	0.05	0.01
16	VLK	0.09	11.30	0.06	0.01
17	TPI	0.11	9.23	0.06	0.01
18	VKT	0.25	3.94	0.02	–
19	VED	0.26	3.86	0.02	–
20	KODI	0.05	0.95	–	–
Average		0.36	6.75	0.11	0.01

concentrations are always higher than  $^{238}\text{U}$  in the locations of PKK, NSI and CPI. This may be due to the fact that uranium dissolves in water and thorium is a particularly insoluble element.

## 10 Conclusion

Activity concentration of radionuclides is determined for sediments using gamma ray spectrometer along the east coast of Tamil Nadu about 5 m distance from seashore line. The average activity ( $40.45 \text{ Bq kg}^{-1}$ ) of  $^{232}\text{Th}$  is slightly higher compared with the world average value

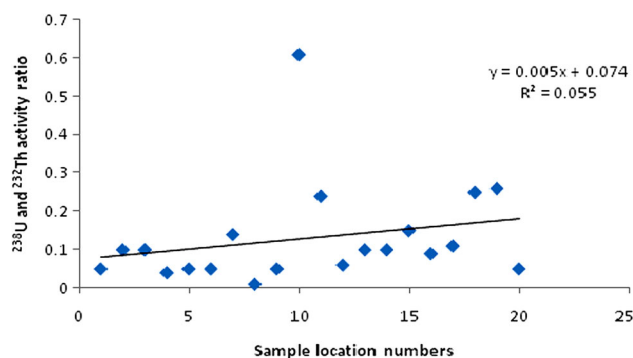


**Fig. 12** Spatial distribution of  $^{238}\text{U}$  and  $^{232}\text{Th}$

( $30 \text{ Bq kg}^{-1}$ ). The average activity concentrations of natural radionuclides ( $^{238}\text{U}$ ,  $^{232}\text{Th}$  and  $^{40}\text{K}$ ) and all calculated radiological parameters are higher than the recommended level in Karaikal. This may be due to the presence of rich black sands which enhances the monozite content in sediments. Moreover, it is also due to the recent development of major industries (in the coastal area and offshore drilling) and minor harbor activities. The results of Pearson correlation, principal component analysis and cluster analysis show that concentration of uranium and thorium mainly contributes in natural radiation in the study area. From the analysis it is concluded that no harmful radiation effects are posed due to the activity of coastal sediment to the public going for recreation on the beaches or the sailors and fisherman in the area due to the activity of coastal sediments.

**Acknowledgements** The author (Dr. R. Ravisankar) express a sincere thanks to Dr. B. Venkataraman, Group director, Health, Safety and Environmental group, Indira Gandhi Centre for Atomic Research Centre, Kalpakkam, Tamil Nadu 603102 to utilize the instrument facilities in laboratory.

## References

- Akram M, Qureshi RM, Ahmad N, Solaija TJ (2006) Gamma-emitting radionuclides in the shallow marine sediments off the Sindh Coast, Arabian sea. *Radiat Prot Dosim* 118:440–447. doi:10.1093/rpd/nci355
- Alatise OO, Babalola IA, Olowofela JA (2008) Distribution of some natural gamma emitting radionuclides in the soils of the coastal areas of Nigeria. *J Environ Radioact* 99:1746–1749. doi:10.1016/j.jenvrad.2008.06.014
- Al-Trabulsi HA, Khater AEM, Habbani FI (2011) Radioactivity levels and radiological hazard indices at the Saudi coast line of the Gulf of Aqaba. *Radiat Phys Chem* 80:343–348. doi:10.1016/j.radphyschem.2010.09.002
- Arogunjo AM, Farai IP, Fuwape IA (2004) Dose rate assessment of terrestrial gamma radiation in the delta region of Nigeria. *Radiat Prot Dosim* 108:73–77. doi:10.1093/rpd/nch010
- Beretka J, Matthew PJ (1985) Natural radioactivity of Australian building materials. *Industrial wastes and by-products. Health Phys* 48:87–95



- Cermak V, Huckenholz HG, Rybach L, Schmid R (1982) Radioactive heat generation in rocks. In: Hellwege K (ed) Landolt–Bornstein numerical data and functional relationships in science and technology. New Series, Group V. Geophysics and Space Research. Springer, Berlin, pp 433–481
- Chandrasekaran A, Ravisankar R, Hari Krishnan N, Satapathy KK, Prasad MVR, Kanagasabapathy KV (2015) Multivariate statistical analysis of heavy metal concentration in soils of Yelagiri Hills, Tamilnadu, India—spectroscopic approach. *Spectrochim Acta Part A Mol Biomol Spectrosc* 137:589–600. doi:10.1016/j.saa.2014.08.093
- de Mora S, Sheikholeslami MR, Wyse E, Azemard S, Cassi R (2004) An assessment of metal contamination in coastal sediments of the Caspian Sea. *Mar Pollut Bull* 48:61–77. doi:10.1016/S0025-326X(03)00285-6
- El-Gamal A, Nasr S, El-TaHER A (2007) Study of the spatial distribution of natural radioactivity in the upper Egypt Nile River sediments. *Radiat Meas* 42:457–465. doi:10.1016/j.radmeas.2007.02.054
- Harb S (2008) Natural radioactivity and external gamma radiation exposure at the coastal Red Sea in Egypt. *Radiat Prot Dosim* 130:376–384. doi:10.1093/rpd/ncn064
- Helbig K, Treitel S (1996) Handbook of geophysical exploration. Seismic Exploration, Amsterdam
- ICRP 60 (1990) Recommendations of the International Commission on Radiological Protection, in ICRP Publication 60, Pergamon Press Annals of the ICRP, Oxford
- Janardhanan (1986) Systematic quaternary geological and geomorphological mapping around Mudukulathur and Paramaguditaluks, Ramanathapuram districts, Tamil Nadu, Unpublished Progress report of GSI
- Kalyani VD, Chandrasekhar Rao MV, Sree Krishna Murty G, Satyanarayana G, Sastry DL, Sahasrabhude SG, Babu DA, Iyer MR (1990) Analysis of <sup>232</sup>Th and <sup>238</sup>U in the beach sands and the ocean sediments. *Indian J Environ Prot* 10:931–934
- Kannan V, Rajan MP, Iyengar MA, Ramesh R (2002) Distribution of natural and anthropogenic radionuclides in soil and beach sand samples of Kalpakkam (India) using hyper pure germanium (HPGe) gamma ray spectrometry. *Appl Radiat Isotopes* 57:109–119. doi:10.1016/S0969-8043(01)00262-7
- Krieger R (1981) Radioactivity of construction materials. *Betonwerk Fertigteil Tech* 47:468–473
- Loveson VJ, Rajamanickam GV, Anbarasu K (1990) Remote sensing application in the study of sea-level variation along the Tamil Nadu coast, India. In: Rajamanickam GV (ed) Sea level variation and its impact on coastal environments. Pub Tamil University, Thanjavur, pp 179–195
- Mohanty AK, Sengupta D, Das SK, Vijayan V, Saha SK (2004) Natural radioactivity in the newly discovered high background radiation area on the eastern coast of Orissa, India. *Radiat Meas* 38:153–165. doi:10.1016/j.radmeas.2003.08.003
- Narayana Y, Somashekarappa HM, Karunakara N, Avadhani DN, Mahesh HM, Siddappa K (2001) Natural radioactivity in the soil samples of Coastal Karnataka of South India. *Health Phys* 80:24–33. doi:10.1097/00004032-200101000-00006
- NEA-OECD (1979) Exposure to radiation from natural radioactivity in building materials. Report by NEA Group of Experts of the Nuclear Energy Agency. OECD, Paris
- Orgun Y, Altinsoy N, Sahin SY, Gungor Y, Gultekin AH, Karaham G, Karaak Z (2007) Natural and anthropogenic radionuclides in rocks and beach sands from Ezine region (Canakkale), Western Anatolia, Turkey. *Appl Radiat Isotopes* 65:739–747. doi:10.1016/j.apradiso.2006.06.011
- Radhakrishna AP, Somashekarappa HM, Narayana Y, Siddappa K (1993) A new natural background radiation area on the southwest coast of India. *Health Phys* 65:390–395. doi:10.1097/00004032-199310000-00006
- Ramasamy V, Senthil S, Meenakshisundaram V, Gajendran V (2009) Measurement of natural radioactivity in beach sediments from North East Coast of Tamilnadu, India. *Res J Appl Sci Eng Technol* 1:54–58
- Rao LR (1956) Recent contributions to our knowledge of the Cretaceous rocks of South India. *Proc Indian Acad Sci Sect B Springer India* 44:185–245. doi:10.1007/BF03052019
- Ravisankar R, Sivakumar S, Chandrasekaran A, Prince PrakashJebakumar J, Vijayalakshmi I, Vijayagopal P, Venkatraman B (2014) Spatial distribution of gamma radioactivity levels and radiological hazard indices in the East Coastal sediments of Tamilnadu, India with statistical approach. *Radiat Phys Chem* 103:89–98. doi:10.1016/j.radphyschem.2014.05.037
- Ravisankar R, Chandramohan J, Chandrasekaran A, Prince PrakashJebakumar J, Vijayalakshmi I, Vijayagopal P, Venkatraman B (2015) Assessments of radioactivity concentration of natural radionuclides and radiological hazard indices in sediment samples from the East coast of Tamilnadu, India with statistical approach. *Mar Pollut Bull* 97:419–430. doi:10.1016/j.marpolbul.2015.05.058
- Rybach L (1988) Determination of heat production rate. Handbook of terrestrial heat flow density determinations. Kluwer, Dordrecht
- Saad HR, Al-Azmi D (2002) Radioactivity concentrations in sediments and their correlation to the coastal structure in Kuwait. *Appl Radiat Isot* 56:991–997. doi:10.1016/S0969-8043(02)00061-1
- Sengupta D, Mohanty AK, Das SK, Saha SK (2005) Natural radioactivity in the high background radiation area at Erasama beach placer deposit of Orissa, India. *Int Congr Ser* 1276:210–211. doi:10.1016/j.ics.2004.12.010
- Sivakumar S, Chandrasekaran A, Ravisankar R, Ravikumar SM, Prince PrakashJebakumar J, Vijayagopal P, Vijayalakshmi I, Jose MT (2014) Measurement of natural radioactivity and evaluation of radiation hazards in coastal sediments of east coast of Tamilnadu using statistical approach. *J Taibah Univ Sci* 8:375–384
- Stephen-Pichaimani V, Jonathan MP, Srinivasalu S, Rajeshwara-Rao N, Mohan SP (2008) Enrichment of trace metals in surface sediments from the northern part of Point Calimere, SE coast of India. *Environ Geol* 55:1811–1819. doi:10.1007/s00254-007-1132-9
- Suresh Gandhi M, Ravisankar R, Rajalakshmi A, Sivakumar S, Chandrasekaran A, PremAnand D (2014) Measurements of natural gamma radiation in beach sediments of north east coast of Tamilnadu, India by gamma ray spectrometry with multivariate statistical approach. *J Radiat Res Appl Sci* 7:7–17. doi:10.1016/j.jrras.2013.11.001
- Tanaskovic I, Golobocanin D, Miljevic N (2012) Multivariate statistical analysis of hydrochemical and radiological data of Serbian spa waters. *J Geochem Explor* 112:226–234. doi:10.1016/j.gexplo.2011.08.014
- Tari M, Zarandi SAM, Mohammadi K, Zare MR (2013) The measurement of gamma-emitting radionuclides in beach sand cores of coastal regions of Ramsar, Iran using HPGe detectors. *Mar Pollut Bull* 74:425–434. doi:10.1016/j.marpolbul.2013.06.030
- Taskin H, Karavus M, Ay P, Topuzoglu A, Hındiroglu S, Karahan G (2009) Radionuclide concentrations in soil and lifetime cancer risk due to the gamma radioactivity in Kirklareli, Turkey. *J Environ Radioact* 100:49–53. doi:10.1016/j.jenvrad.2008.10.012
- UNSCEAR, United Nations Scientific Committee on the Effects of Atomic Radiation (1988) Sources, effects and risks of ionizing radiation. United Nations, New York
- UNSCEAR, United Nations Scientific Committee on the Effects of Atomic Radiation (1993) Sources, effects and risks of ionizing radiation. United Nations, New York



- UNSCEAR, United Nations Scientific Committee on the Effects of Atomic Radiation (2000) Sources, effects and risks of ionizing radiation. Report to the General Assembly with annex B. United Nations, New York
- Uosif MAM, El-Taher A, Abbady GE (2008) Radiological significance beaches and used for climate therapy from Safaga, Egypt. *Radiat Prot Dosim* 131:331–339. doi:[10.1093/rpd/ncn175](https://doi.org/10.1093/rpd/ncn175)
- Zare MR, Mostajaboddavati M, Kamali M, Abdi MR, Mortazavi MS (2012)  $^{235}\text{U}$ ,  $^{238}\text{U}$ ,  $^{232}\text{Th}$ ,  $^{40}\text{K}$  and  $^{137}\text{Cs}$  activity concentrations in marine sediments along the northern coast of Oman Sea using high-resolution gamma-ray spectrometry. *Mar Pollut Bull* 64:1956–1961. doi:[10.1016/j.marpolbul.2012.05.005](https://doi.org/10.1016/j.marpolbul.2012.05.005)